EXPERIMENTAL VALIDATION OF THE HYBRID AIRFOIL DESIGN PROCEDURE FOR FULL-SCALE ICE ACCRETION SIMULATION

Farooq Saeed,* Michael S. Selig† and Michael B. Bragg‡
Department of Aeronautical and Astronautical Engineering
University of Illinois at Urbana-Champaign, Urbana, Illinois 61801-2935

Harold E. Addy, Jr.§
NASA Lewis Research Center
21000 Brookport Road, Cleveland, Ohio 44135-3191

ABSTRACT

This paper presents results from the first series of ice accretion tests performed to validate the hybrid airfoil design method of Saeed, et al. The hybrid airfoil design method was developed to facilitate the design of hybrid or subscale airfoils with full-scale leading edges and redesigned aft-sections that exhibit full-scale airfoil water droplet impingement characteristics throughout a given α−range. The formulation is based on the assumption that the leading-edge ice accretion will be the same between the full-scale and hybrid airfoils if droplet cloud properties, droplet impingement, local leading-edge flowfield, model surface geometry, model surface quality, and model surface thermodynamic characteristics are the same. Thus, if ice accretion simulation could be predicted in terms of the droplet impingement characteristics alone, a myriad of issues related to ice accretion scaling could be avoided for tests where leading-edge ice accretion is desired.

Hence, the method was used to design a 2-D half-scale hybrid airfoil, with a 20% plain-flap and a 5% upper and 20% lower leading-edge surface of an a scaled down model of a modern business jet wing section, that simulates droplet impingement characteristics of the scaled business jet airfoil, on- and off-design. The 2-D scaled business jet airfoil model and its half-scale hybrid airfoil model were then subjected to icing tests in the NASA Lewis Icing Research Tunnel (IRT). The design as well as the icing test conditions selected for the tests were representative of the conditions the business jet wing section would experience in flight.

This paper presents a comparison between the actual ice shapes that formed on the scaled business jet and hybrid airfoil models during the tests. A comparison between the actual ice shapes and those predicted by LEWICE 1.6 under similar conditions is also shown. The results from the initial series of validation tests are encouraging enough to suggest that the method has great application potential.

NOMENCLATURE

C_d	= airfoil drag coefficient
C_p	= pressure coefficient
c	= airfoil chord length
LWC	= liquid water content
M	= freestream Mach number
P	= pressure
Re	= freestream Reynolds number, $\rho Uc/\mu$
T	= temperature
U	= airspeed
MVD	= median volumetric droplet diameter
α	= angle of attack relative to the chord line
α_e	= effective angle of attack relative to the nose section chord line, $\alpha - \gamma$
γ	= nose droop angle
μ	= air viscosity
ρ	= air density

Subscripts:

s	= static
t	= total
ws	= wake survey

INTRODUCTION

There is a growing concern among the aeronautical engineering community to better understand the process of ice accretion. This concern is largely due to a number of icing related accidents[1] in recent years. In order to improve flight safety, a better understanding of the effect of ice accretion on the aerodynamic performance of airfoils or wings is required. Since the physics of ice accretion is not understood very well, computer simulations that can show exactly what effect the ice accretion would have on a particular design, or predict whether the aircraft is safe to fly under certain weather conditions, or even

* Graduate Research Assistant. Student Member AIAA.

† Assistant Professor. Senior Member AIAA.

‡ Professor. Associate Fellow AIAA.

§ Aerospace Engineer, Icing Branch, NASA Lewis Research Center. Member AIAA.

suggest what can be done to make it safer, are still in their infancy. An important alternative to accurate simulation would be to evaluate the aerodynamic performance of the airfoil sections, or the wing as a whole, at the icing conditions within the certification icing envelop resulting in the largest performance penalties — test results that can then be used for avoidance of condition critical to the safety of flight. The determination of the critical ice accretion and its aerodynamic effect on a set of modern airfoils, typical of those in use on current aircraft, is underway at NASA Lewis Research Center. The research reported here is part of this larger effort.

Owing to the difficulties and uncertainties in ice accretion scaling,[2–10] testing at full-scale is desirable, yet costly. Moreover, available ice accretion tunnels are too small to test full-scale airfoils or wings of most aircraft of interest. Since aircraft wing ice accretion depends, most importantly, on the airfoil leading-edge geometry[11] where the ice first accretes, one way to expand the usefulness of existing icing tunnels and to facilitate testing of aircraft deicing/anti-icing systems is to test "hybrid airfoils" or "sub-scale airfoils" with full-scale leading edges and redesigned aft sections to provide full-scale icing conditions at the leading edge. The term "hybrid method" refers to using a full-scale leading edge to match the full-scale ice accretion. The aft section of the hybrid airfoil is specially designed to provide flowfield and droplet impingement similar to that on the full-scale airfoil leading-edge. In an early work by Glahn,[12] airfoils with full-scale leading edges and truncated aft-sections were used to simulate the flowfield of the full-scale, thereby avoiding the associated scaling issues. Interestingly, neither the approach nor its range of application received much attention despite its numerous merits.

In the absence of a systematic study to provide insight into the design of the aft section, a more recent study[13] was carried out in which a design procedure for hybrid airfoils was successfully developed and demonstrated with specific design examples. The formulation was, however, based on the assumption that the leading-edge ice accretion will be the same between the full-scale and hybrid airfoils if the icing cloud properties, droplet-impingement characteristics, local nose-section flowfield, model surface geometry, model surface quality, and model surface thermodynamic characteristics are the same. The study showed that hybrid airfoils could be designed to exhibit both the full-scale flowfield on its nose section as well as full-scale droplet-impingement characteristics. The results of the study were implemented into a hybrid airfoil design and analysis code that utilizes validated computational airfoil aerodynamics and droplet-impingement codes.[14–16]

A limitation of the design procedure presented in Ref. 13 is its restriction to single-point design and, therefore, lacks the capability to handle off-design cases. To overcome this limitation, a more recent study[17] was carried out with the objective to expand the scope of the single-point design procedure[13] to a method that enables the hybrid airfoils to exhibit both the full-scale local nose-section flowfield as well as droplet-impingement characteristics throughout a desired α-range. The results of the study indicate that, although, a flap can be used very effectively to achieve full-scale droplet-impingement characteristics at off-design angles of attack α, the use of a flap, however, does not simulate full-scale flowfield on the nose section to an accuracy similar to that for the single-point design case. Since the difference in the local nose-section flowfield will affect the thermodynamics of ice accretion as the droplets impinge on the surface, it was suspected that ice accretion simulation may be compromised.

Hence, it becomes necessary to establish the validity of the basic assumption upon which both of these methods[13,17] were formulated, namely, the assumption that the leading-edge ice accretion will be the same between the full-scale and hybrid airfoils if droplet cloud properties, droplet impingement, local leading-edge flowfield, model surface geometry, model surface quality, and model surface thermodynamic characteristics are the same, through extensive ice accretion tests. Thus, a series of ice accretion tests were planned as part of the on-going research effort in support of NASA's Modern Airfoil Ice Accretion program.[18]

For this purpose, an airfoil similar to that found on a modern business jet main wing section, shown in Fig. 1a, was provided by NASA. The hybrid airfoil design method[13,17] was then used to design a half-scale hybrid airfoil, shown in Fig. 1b, with a 20% plain-flap and a 5% upper and 20% lower full-scale surface of the modern business jet airfoil leading edge that simulates droplet impingement characteristics of the modern business jet airfoil, both on- and off-design. The 2-D modern business jet and hybrid airfoil models were built at NASA Lewis for ice accretion tests in the NASA Lewis Icing Research Tunnel (IRT) for the present and a related[18] study. The design as well as the icing test conditions were selected from the FAR Appendix C envelope and reflect those that a modern business jet would encounter.

The focus of this paper is, therefore, to present the results of the ice accretions test and discuss the

true merits of the hybrid airfoil design method[13,17] through a comparison of theoretical and experimental results. The paper also presents the ice shapes predicted by the NASA Lewis ice accretion prediction code LEWICE[19] for comparison with the experimental ice shapes.

In the sections that follow, the details of the experimental method are presented followed by a results and discussion section. Finally, the paper presents some important conclusions.

EXPERIMENTAL METHODS

The experiments were performed in the NASA Lewis Icing Research Tunnel (IRT). The IRT is the world's largest refrigerated icing tunnel, capable of generating icing conditions encountered by aircraft. Detailed information regarding the test facility can be found in Ref. 20. A brief description of the test facility and the icing tests performed to validate the hybrid airfoil design method,[13,17] in particular, are as follows.

The Test Facility

The IRT is a closed-loop atmospheric-type tunnel for tests of low-speed models. The tunnel is operated by an interactive computer control system that provides monitoring and recording of test data with 500 data channels. The test section is 6-ft high, 9-ft wide, and 20-ft long. Airspeeds in the empty test section can be varied from 45 to 260 kts (50 to 300 mph). The tunnel is operated at atmospheric pressure, and the air temperature range is controlled from ambient temperature to $-20 \pm 1°$ F.

At 11.5 ft from the inlet of the test section is a 8.6-ft diameter turntable. The turntable can rotate $\pm 20°$ horizontally and is used for mounting test models. Typically, 2-D models are installed vertically in the tunnel, spanning the tunnel height. The balance chamber encloses both the test section and control room and shares the same static pressure as the test section. Drag can also be measured using a traversing wake-survey probe.

Ten spray bars containing atomizing nozzles are used to develop a uniform test-section icing cloud. The nozzles produce water droplets of MVD's between 15 and 40 microns with LWC from 0.5 to 2.5 g/m^3.

Four viewing windows (three of which are electrically heated) between the control room and the test section allow the use of photographic, video and flow visualization equipment for recording visual data.

Model Description

The modern business jet airfoil and the hybrid airfoil models were built as 2-D models with a span of 72 inches and fabricated specifically for vertical installation in the IRT. In the sections that follow, the modern business jet main wing section is referred to as the "full-scale" airfoil. The full-scale and the hybrid models have a chord of 36 and 18 inches, respectively. (It should be noted that the 36-in. chord modern business jet airfoil is not the full-scale. Rather, the 18-in. hybrid airfoil was designed to simulate icing on the so-called full-scale 36-in. airfoil model for validation of the methodology.) The full-scale airfoil model was fabricated as part of NASA's Modern Airfoil Ice Accretion program.[18] The same model was, therefore, utilized in the design studies[13,17] as well in the validation tests to save additional expense. For details regarding the full-scale business jet airfoil model, the reader is referred to Ref. 18. The details of the half-scale hybrid model are as follows.

The hybrid model was made in three separate sections: the leading edge (nose section), the main body, and a 20% chord movable flap. The leading edge, which covered 15% of the suction surface and 40% of the pressure surface, was made of fiberglass in a fashion similar to the full-scale model.[15] This was done to ensure that conduction heat transfer and surface characteristics remained the same for the two models. The main body was made of 7370 aluminum with a T351 temper. It was made in two separate halves that intersected at the chord line of the model. This allowed the pressure instrumentation to be placed inside the model. Twenty-eight surface static pressure orifices were built into the model around its leading edge and across both surfaces of the main body. The orifices were located along a chord line on the model 30 inches above the tunnel floor when installed in the IRT. The movable flap was also made of 7370 aluminum with T351 temper. It was attached to the main body by four simple, straight, steel hinges.

A flap actuator, consisting of a rotary motor and an actuator arm, was used to deflect the flap remotely. An electric sensor was used for recording the flap deflection as well as for setting its position. Both the actuator and the sensor were attached to the turntable and adequately shielded from direct airflow.

Model Accuracy

To determine the accuracy of the hybrid airfoil model profile, its digitized coordinates were compared with the coordinates of the true (design) airfoil. The comparison is shown in Fig. 2, which indicates differences in the upper (solid line) and lower (dashed line) surfaces. A displacement above or below the x-axis indicates that the true coordinates lie

above or below the model coordinates, respectively. Since the displacement of both lines is mostly above the axis, (which is also apparent from the overlay plot in Fig. 2) one can infer that the model airfoil has a different camber than the true airfoil. Moreover, the maximum displacements are occurring at the 15%c and 40%c locations on the upper and lower surfaces, respectively. Since the leading edge section covers this region of the model airfoil, one concludes that the leading edge or the nose section was not aligned correctly with the main body of the model during installation. Overall, the average difference between the two profiles was approximately 0.022 in.

Figure 3 shows the full-scale and the two hybrid airfoil (design and model) profiles such that their nose sections coincide. In this figure, the values 3.00 deg and 2.27 deg represent the angle between the full-scale chord and the design and model airfoil chords, respectively, and represent the amount of the nose droop.[13] Figure 3, therefore, confirms the fact that the nose section of the hybrid model was installed incorrectly during its construction and, moreover, that the nose section is misaligned approximately 0.73 deg.

As it will be shown later, the misalignment of the nose-section of the hybrid airfoil profile results in the disagreement between experimental data and theoretical (design) predictions. However, an analysis of the hybrid model (as tested) with the aid of the hybrid airfoil design code shows results which are in good agreement with the experimental data. For the analysis of the hybrid model, it was necessary to determine the correct angle of attack relative to the common leading edge or nose section of the full-scale and the hybrid models.

Test Instrumentation

A wake survey system was used to obtain a measure of airfoil section drag. This system consisted of a movable Pitot probe that traversed the model wake at mid-span and at a distance of three chords downstream of the model. Freestream conditions were measured using the facility Pitot-static probe located five chords upstream of the model near the tunnel wall. Total pressures were measured using absolute pressure transducers while static pressures were measured using differential pressure transducers. The probe position was electronically sensed.

Surface pressure measurement were recorded only during dry runs. During the ice accretion tests the pressure taps were covered with a thin tape to prevent the introduction of water into the pressure tubes. A total of 28 surface static pressure taps were built into the hybrid model as compared with 44 on the full-scale model because of the presence of the flap.

Flow visualization was used to observe the onset of flow separation during model the icing tests. Flow cones from X-Aero System, Inc. in Seattle, WA were employed for this task. A flow cone is a white plastic cone 1-3/4 in. long and 9/32 in. in diameter at its base. The cones were attached to the model via a 1-3/4 in. length of string emanating from the cones apex. An inch wide aluminum tape was applied over the string near the cones apex to affix the cone to the model. The extra string was doubled back and taped over with 2 in. wide aluminum tape. A row of cones was affixed to the model in a chordwise direction on the suction surfaces at approximately 18 in. from the tunnel floor. Video cameras and recorders were used to observe and record the flow over the model surface and the cones and to detect the onset of flow separation.

Test Conditions

The conditions chosen for the design of the hybrid airfoil as well as the validation tests were representative of the FAR Appendix C envelope as well as those that the business jet wing section (full-scale airfoil) would experience. Table 1 lists the flight and icing conditions that were selected for the design of the half-scale hybrid airfoil model, whereas, Tables 2 and 3 list the conditions at which the actual ice accretion tests were performed. It should be noted that the angle of attack values appearing in Tables 2 are relative to the airfoil chord line (α) and that those appearing in Table 3 are relative to the nose section chord line (α_e). The reason is that the hybrid airfoil was designed with a nose section identical to the full-scale airfoil but with a nose droop[13] of $\gamma = -3$ deg. And, therefore, in order to keep the same angle of attack relative to its nose section as the full-scale airfoil, the hybrid airfoil was tested at an angle of attack 3 deg higher than the corresponding full-scale test.

Test Description

A typical test run consisted of several steps. First the model was set at the given attitude. (Airfoil attitude is the angle of the chord of the airfoil with respect to the tunnel centerline.) After the approximate airspeed was reached, the flap was set to the desired position. The tunnel airspeed was adjusted to account for the change as a result of flap deflection. Then the tunnel air and model were brought to the desired operating temperature. A wake survey was then conducted to measure the clean airfoil drag. The model was then subjected to the predetermined icing conditions for the specified amount of

time. After the icing cloud was terminated, another wake survey was taken and recorded. The tunnel fan was then brought to a stop such that detailed records of the ice shape could be made.

Photographs of the accreted ice were taken with a 35-mm camera. Then the ice was cut, using a warm aluminum template, in three spanwise locations: 30 in., 36 in., and 42 in. from the floor, so that hand tracings using a pencil and cardboard template could be made of the ice shape profile. The ice thickness was measured at each of these cuts using a depth gage. Typically, two ice depth measurements were made at each cut: a suction surface maximum and a pressure surface maximum ice thickness. The ice was then cleaned off the model and the tunnel cleared for the next test run.

RESULTS AND DISCUSSION

In this section, the results of the icing tests are presented. A total of 49 ice accretion tests were conducted for this study which included 11 ice accretion tests on the business jet (full-scale) airfoil model. In addition, 27 surface pressure measurement tests were conducted on the hybrid model as well. Surface pressure data for the full-scale model was taken as part of NASA's Modern Airfoil Ice Accretion program.[18] Although a multitude of data was recorded during the tests, the data presented here has been restricted to the results that are pertinent to the validation of the hybrid airfoil design method.[13,17] Therefore, only the significant ice shape data has been included in this paper.

First, the repeatability and accuracy of the experimental results is discussed. Then the hybrid model ice shapes are shown in comparison with the full-scale model ice shapes to determine the flap deflection that best simulates the full-scale ice accretion. The optimum flap deflection is determined for each angle of attack case and is then compared with the theoretical predictions. A comparison of results from the NASA Lewis ice accretion code LEWICE[19] is also presented and compared with the test results.

As mentioned earlier, the misalignment of the hybrid-airfoil nose section resulted in a disagreement between experimental data and theoretical predictions. However, an analysis of the hybrid model (as tested) with the aid of the hybrid airfoil design code shows that in fact the disagreement is due to the misalignment of the nose section that leads to an incorrect interpretation of the angle of attack values reported in the tests. A correction to the angle of attack values yields results that are in good agreement with the experimental data.

Experimental Repeatability and Accuracy

Several icing tests were repeated to determine the repeatability of the ice shapes and the corresponding drag forces based on the wake survey data. Figures 4a and 4b show a comparison of the ice shape tracings from separate icing test runs under similar tests conditions for the full-scale and the hybrid models, respectively. Overall, the repeatability of ice shapes was observed to be as good as shown in Fig. 4a. Reference 21 indicates that the amount of ice shape variability, as shown in Fig. 4a, is typical. However, a few odd cases, such as Run 501 in Fig. 4b, were also encountered.

Repeatability of the section drag coefficients, as measured by the wake survey system, was also found to be good (within ±5%). The results for the test cases of Fig. 4a are shown in Fig. 5. Figure 6 shows a comparison of the total pressure deficit in the wake between the clean and iced full-scale airfoil for the same test conditions. As obvious from Fig. 6, the amount of ice accretion can have a tremendous effect on the size of the airfoil wake. It, therefore, becomes questionable whether standard wind tunnel corrections[22] can adequately account for wake blockage.

Experimental Ice Shapes

The experimental ice shape tracings are shown in Figs. 7a through 7d for different angle of attack conditions. The figures show the effectiveness of a flap in varying the ice accretion and, therefore, indicate its usefulness in simulating full-scale ice accretions. As evident from these results, the ice shapes are sensitive even to small changes (±2 deg) in the flap deflection. An explanation of the results can be given in terms of the airfoil circulation.

The amount of circulation, which is governed by both the angle of attack and flap deflection, plays a dominant role in determining the impingement characteristics through its impact on the flowfield, and therefore, the ice accretion. In Figs. 7a through c, an increase in flap deflection resulted in an increase in circulation since the upper surface limit of the accreted ice mass is displaced towards the leading edge due to the movement of the front stagnation point. However, in Fig. 7d, the opposite is true. This is indicative of an already stalled hybrid airfoil since a decrease in flap deflection is causing the upper extent of ice accretion to move forward signifying a rearward movement of the stagnation point and, hence, an increase in circulation. The overlap and sometimes even a crossover of ice shape tracings can be attributed to the odd cases (Fig. 4b Run 501) that were encountered during the tests.

Figure 8 shows the plot of hybrid airfoil ice shapes that best simulate the corresponding full-scale airfoil ice shapes for the specified test conditions. This has been shown to indicate the optimum flap deflection on hybrid airfoils that best simulate the corresponding actual full-scale ice shape for a given test condition in the IRT.

Ice Shape Prediction Using LEWICE

LEWICE[19] is an ice accretion prediction code that uses a time-stepping procedure to determine the shape of ice accretion. LEWICE Version 1.6 was run to determine the strength and weaknesses of the code for use in the hybrid airfoil design process. The LEWICE code was run with the IRT tunnel conditions, the geometry of the model (as tested) and input flags that allowed control over the number of time steps to be used for simulation. Specifically, the IFLO[19] parameter was set equal to 4 in all the cases reported in this paper on the basis of a parametric study that showed that IFLO = 4 produced results that were more consistent with experiments. For details regarding important parameters and other features of the LEWICE code, the reader is referred to the most recent update to the User's Manual.[19]

The full-scale and hybrid model airfoils (as tested) were analyzed using the LEWICE code to determine the optimum flap deflections on the hybrid airfoil that best simulate the full-scale predicted ice shapes for a given test condition. These analyses included almost all of the test conditions indicated in Tables 2 and 3. Some of the significant results are shown in Fig. 9, which is similar to Fig. 8 except that in Fig. 9 the results from the LEWICE code have also been included for comparison with the experiment.

The results from the LEWICE code represent the cases that best simulate the predicted full-scale ice shapes. It is encouraging to note that the LEWICE code predicts optimum flap deflections that are in good agreement with the experimentally observed values. This is in spite of the fact that the predicted ice shapes are quite different than the experiments. The reason lies in the fact that the LEWICE code in its present stage is unable to accurately model conditions that are favorable for glaze or even mixed ice accretion which are representative of the test conditions that were selected for the present study.

Flow and Droplet Impingement Analysis of the Hybrid Model Airfoil

In an earlier section of this paper, it was shown that not only was the hybrid model's profile different but also its attitude with the horizontal axis when its nose section was aligned with that of the full-scale or the true airfoil as design (see Fig. 3). The reasons for aligning the nose section were to 1) show that the hybrid airfoil has the same nose section profile as that of the full-scale airfoil from which it has been derived and 2) to indicate that the hybrid airfoil has a nose droop ($\gamma = -3$ deg) and in order to keep the angle of attack of the flow relative to its nose section the same as the full-scale the airfoil should be analyzed at $\alpha_e = \alpha - \gamma$.

Figure 3 indicates that the trailing-edge of the model airfoil is at a lower angle of attack α_e value (by approximately 0.73 deg) when the nose sections are aligned with the flow. Assuming that the nose sections were aligned during the tests, then a comparison of surface pressure distribution between experiment and that predicted by XFOIL[15] should confirm that the above correction is required in interpreting the angle of attack values.

For this purpose, the model-airfoil surface-pressure distributions were determined at two different angles of attack, i.e., at $\alpha_e = 9.0$ and 8.28 deg, and at $Re = 3$ million, $M = 0.28$ using XFOIL. The results are shown in Fig. 10 in comparison with the surface pressure data taken during the icing test at the test conditions: Attitude = 9 deg, $Re = 3$ million and $M = 0.28$. The results indicate that the pressure distribution corresponding to $\alpha_e = 9.0$ deg is in better agreement with the test data. It, therefore, suggests that the angles of attack referred to in the test data pertaining to the hybrid airfoil are relative to the model chord and, therefore, the analysis of the model should be performed at $\alpha_e = 9.0$.

Since the hybrid-model chord is at a lower angle of attack (Fig. 3), the above discussion suggests that the droplet impingement analysis of the hybrid model should be performed at $\alpha_e = \alpha - \gamma$, where $\alpha = \alpha_u + 0.73$ deg and $\gamma = -3$ deg, for a comparison with the experimental results. This is confirmed by the droplet impingement analysis of the hybrid-model airfoil using the hybrid airfoil design code. Figures 11a and 11b show the comparison of the optimum flap deflection required to match full-scale airfoil droplet impingement between the hybrid-model analyses and the experiment when the analyses are performed at $\alpha_e = 8.28$ deg. A general disagreement is found to exist. The analysis of the design is, however, at $\alpha_e = 9.0$ deg and have been included in the figure to indicate the difference between the model and the true airfoil (design). In Fig. 11b, the hybrid-model airfoil is analyzed at $\alpha_e = 9.0$ deg. The results are then found in good agreement with the experiment and suggest that it is possible to simulate full-scale ice accretion using subscale hybrid airfoils.

CONCLUSIONS

In conclusion, several important observations can be drawn from the validation tests. The most important, however, is that hybrid airfoils can be used to simulate full-scale ice accretion over a range of angle-of-attack conditions. The tests also confirm that the formulation of the hybrid airfoil design procedure based on the assumption that the leading-edge ice accretion will be the same between the full-scale and hybrid airfoils if icing cloud properties, droplet impingement, local leading-edge flowfield, model surface geometry, model surface quality, and model surface thermodynamic characteristics can be used for the design of such hybrid airfoils that simulate full-scale ice accretions. This is true in spite of the fact that the tests were conducted in glaze ice conditions which result in the largest degradation of airfoil performance and that a 12 minute time interval was selected for each test run. (On the average the airfoil models were observed to stall between 1–2 minutes.)

The results also indicate the usefulness of a flap system in simulating full-scale droplet impingement characteristics as well as ice accretions. The use of flap should, however, be restricted to low and moderate angles of attack since at high absolute angles of attack together with high flap deflections, the hybrid airfoils become susceptible to flow separation. This limitation can, however, be overcome by the use of a more sophisticated flap system or by the application of boundary-layer control methods.

The results from the initial series of validation tests are encouraging enough to suggest that the method has great application potential and that it provides an alternate to icing scaling laws. Or the method can be combined with traditional icing scaling methods to reduce the overall scale of the test models even smaller.

ACKNOWLEDGMENTS

This work has been sponsered by NASA Lewis Research Center under grant NCC3-408. Helpful discussions with Tom Ratvasky and Tom Bond of NASA Lewis are gratefully acknowledged. We would like to thank Dave Sheldon and the IRT staff for their valuable advice and assistance throughout the ice accretion tests. Also, we would like to thank Dr. William Wright for his guidance in the use of the NASA Lewis LEWICE code.

REFERENCES

[1]Bragg, M. B.,"Aircraft Aerodynamic Effects Due to Large Droplet Ice Accretions," AIAA Paper 96-0932, Jan. 1996.

[2]Hauger, H. H. and Englar, K. G., "Analysis of Model Testing in an Icing Wind Tunnel," Douglas Aircraft Co., Inc., Rep. No. SM 14993, May 1954.

[3]Sibley, P. J. and Smith, R. E., Jr. "Model Testing in an Icing Wind Tunnel," Lockheed Aircraft Corp., Inc., Rep. No. LR 10981, Oct. 14, 1955.

[4]Dodson, E. D., "Scale Model Analogy for Icing Tunnel Testing," Boeing Airplane Company, Transport Division, Document No. D66-7976, Mar. 1962.

[5]Bragg, M. B., Gregorek, G. M., and Shaw, R. J., "An Analytical Approach to Airfoil Icing," AIAA Paper 81-0403, Jan. 1981.

[6]Ruff, G. A., "Verification and Application of the Icing Scaling Equations," AIAA Paper 86-0481, Jan. 1986.

[7]Bilanin, A. J., "Proposed Modifications to Ice Accretion/Icing Scaling Theory," AIAA Paper 88-0203, Jan. 1988.

[8]Anderson, D. N., "Rime-, Mixed- and Glaze-Ice Evaluations of Three Scaling Laws," AIAA Paper 94-0718, Jan. 1994.

[9]Anderson, D. N., "Methods for Scaling Icing Test Conditions," AIAA Paper 95-0540, Jan. 1995. Also published as NASA TM 106827.

[10]Anderson, D. N., "Further Evaluation of Traditional Icing Scaling Methods," AIAA Paper 96-0633, Jan. 1996. Also published as NASA TM 107140.

[11]Bragg, M. B., "Effect of Geometry on Airfoil Icing Characteristics," *Journal of Aircraft*, Vol. 21, No. 7, Jul. 1984, pp. 505–511.

[12]Glahn, U. H. von, "Use of Truncated Flapped Airfoils for Impingement and Icing Tests of Full-Scale Leading-Edge Sections," NACA RM E56E11, Jul. 1956.

[13]Saeed, F., Selig, M. S.,and Bragg, M. B., "Design of Subscale Airfoils with Full-Scale Leading Edges for Ice Accretion Testing," *Journal of Aircraft*, Vol. 34, No. 1, Jan.–Feb. 1997, pp. 94–100. Also AIAA Paper 96-0635.

[14]Bragg, M. B., "Rime Ice Accretion and Its Effect on Airfoil Performance," Ph. D. Dissertation, Ohio State University, Columbus, Ohio, 1981; see also NASA CR 165599, March 1982.

[15]Drela, M., "XFOIL: An Analysis and Design System for Low Reynolds Number Airfoils," *Lecture Notes in Engineering: Low Reynolds Number Aerodynamics*, T. J. Mueller (ed.), Vol. 54, Springer-Verlag, New York, June 1989, pp. 1–12.

[16]Selig, M. S., and Maughmer, M. D., "A Multipoint Inverse Airfoil Design Method Based on Conformal Mapping," *AIAA Journal*, Vol. 30, No. 5, 1992, pp. 1162–1170.

[17]Saeed, F., Selig, M. S. and Bragg, M. B., "Hybrid Airfoil Design Method to Simulate Full-Scale Ice Accretion Throughout a Given α-Range," to appear in *Journal of Aircraft*, Vol. 35, No. 1, Jan.–

Feb. 1998. Also AIAA Paper 97-0054.

[18]Addy, Jr., H. E., Potapczuk, M. G., and Sheldon, D. W., "Modern Airfoil Ice Accretions," NASA TM 107423, Mar. 1997. Also AIAA Paper 97-0174.

[19]Wright, W. B., "User Manual for the Improved NASA Lewis Ice Accretion Code LEWICE 1.6," NASA CR 198355, June 1995.

[20]Soeder, R. H., Sheldon, D. W., Andracchio, C. R., Ide, R. F., Spera, D. A., and Lalli, N. M., "NASA Lewis Icing Research Tunnel User Manual," NASA TM 107159, June 1996.

[21]Shin, J. and Bond, T. H., "Repeatability of Ice Shapes in the NASA Lewis Icing Research Tunnel," *Journal of Aircraft*, Vol. 31, No. 5, 1994, pp. 1057–1063.

[22]Rae, Jr., W. H., and Pope, A., "*Low Speed Wind Tunnel Testing*," John Wiley & Sons, 2nd Ed., 1984, pp. 344–444.

Table 1 Design flight and icing conditions

Variable	Full scale	Hybrid
U, kts	175	175
T_s, deg F	22.4	22.4
Re	6×10^6	3×10^6
M	0.28	0.28
c, in.	36.0	18.0
MVD, micron	20	20
α, deg	6	6
γ, deg	0	-3
α_e, deg	6	9

Table 2 Flight and icing conditions used for ice accretion tests on the scaled business jet airfoil model.

No.	Run No.	M	U (kts)	α (degrees)	T_s (deg F)	T_t (deg F)	MVD (micron)	LWC (g/m^3)	P_{air} (psig)	Spray time (min.)
1	301	0.28	175	6	13.4	20.823	20	0.43	11.6	6
2	302	0.28	175	4	13.4	20.823	20	0.43	11.6	6
3	303	0.28	175	6	22.4	29.964	20	0.54	16	6
4	304	0.28	175	4	22.4	29.964	20	0.54	16	6
5	305	0.28	175	8	22.4	29.964	20	0.54	16	6
6	306	0.28	175	6	22.4	29.964	20	0.54	16	12
7	307	0.28	175	4	22.4	29.964	20	0.54	16	12
8	308	0.28	175	8	22.4	29.964	20	0.54	16	12
9	309/306r1	0.28	175	6	22.4	29.964	20	0.54	16	12
10	310	0.28	175	2	22.4	29.964	20	0.54	16	12
11	311	0.28	175	0	22.4	29.964	20	0.54	16	12

Table 3 Flight and icing conditions used in actual ice accretion tests on the hybrid business jet airfoil model.

No.	Run No.	M	U (kts)	α_e (degrees)	Flap (degrees)	T_s (deg F)	T_t (deg F)	MVD (micron)	LWC (g/m^3)	P_{air} (psig)	Spray time (min.)
1	501	0.28	175	9	4	22.4	29.964	20	0.54	16	12
2	502	0.28	175	9	2	22.4	29.964	20	0.54	16	12
3	503	0.28	175	9	0	22.4	29.964	20	0.54	16	12
4	504	0.28	175	9	-2	22.4	29.964	20	0.54	16	12
5	505	0.28	175	9	-4	22.4	29.964	20	0.54	16	12
6	506	0.28	175	9	-8	22.4	29.964	20	0.54	16	12
7	507	0.28	175	9	8	22.4	29.964	20	0.54	16	12
8	501r1	0.28	175	9	4	22.4	29.964	20	0.54	16	12
9	503r1	0.28	175	9	0	22.4	29.964	20	0.54	16	12
10	511	0.28	175	7	3	22.4	29.964	20	0.54	16	12
11	512	0.28	175	7	0	22.4	29.964	20	0.54	16	12
12	513	0.28	175	7	-3	22.4	29.964	20	0.54	16	12
13	514	0.28	175	7	-6	22.4	29.964	20	0.54	16	12
14	515	0.28	175	7	-9	22.4	29.964	20	0.54	16	12
15	511r1	0.28	175	7	3	22.4	29.964	20	0.54	16	12
16	501r2	0.28	175	9	4	22.4	29.964	20	0.54	16	12
17	521	0.28	175	11	6	22.4	29.964	20	0.54	16	12
18	522	0.28	175	11	0	22.4	29.964	20	0.54	16	12
19	523	0.28	175	11	-6	22.4	29.964	20	0.54	16	12
20	524	0.28	175	11	12	22.4	29.964	20	0.54	16	12
21	531	0.28	175	5	0	22.4	29.964	20	0.54	16	12
22	532	0.28	175	5	-4	22.4	29.964	20	0.54	16	12
23	533	0.28	175	5	-8	22.4	29.964	20	0.54	16	12
24	534	0.28	175	5	-12	22.4	29.964	20	0.54	16	12
25	505r1	0.28	175	9	-4	22.4	29.964	20	0.54	16	12
26	541	0.28	175	9	0	4.4	11.682	20	0.37	10	18
27	542	0.28	175	9	-4	4.4	11.682	20	0.37	10	18
28	543	0.28	175	9	-8	4.4	11.682	20	0.37	10	18
29	542m	0.28	175	9	-4	4.4	11.682	20	0.37	10	18
30	514r1	0.28	175	7	-6	22.4	29.964	20	0.54	16	12
31	505r2	0.28	175	9	-4	22.4	29.964	20	0.54	16	12
32	504r1	0.28	175	9	-2	22.4	29.964	20	0.54	16	12
33	505r3	0.28	175	9	-4	22.4	29.964	20	0.54	16	12
34	533r1	0.28	175	5	-8	22.4	29.964	20	0.54	16	12
35	535	0.28	175	5	-16	22.4	29.964	20	0.54	16	12
36	533r2	0.28	175	5	-8	22.4	29.964	20	0.54	16	12
37	514r2	0.28	175	7	-6	22.4	29.964	20	0.54	16	12
38	534r1	0.28	175	5	-12	22.4	29.964	20	0.54	16	12

r# - repeat case and number, m - ice-shape mold case

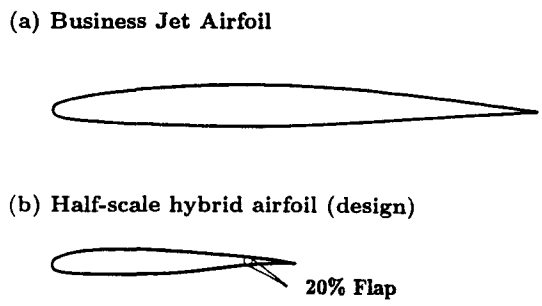

Fig. 1 The scaled business jet airfoil and its half-scale hybrid airfoil.

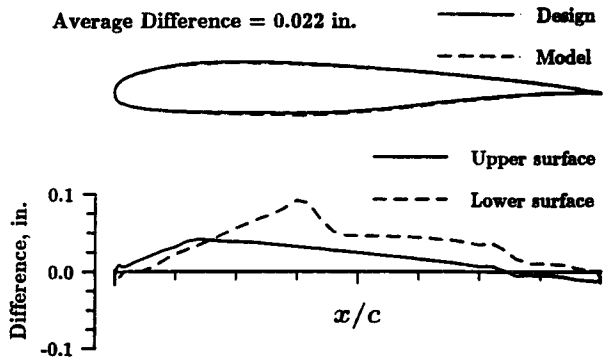

Fig. 2 Hybrid airfoil model accuracy plot (18 in. chord).

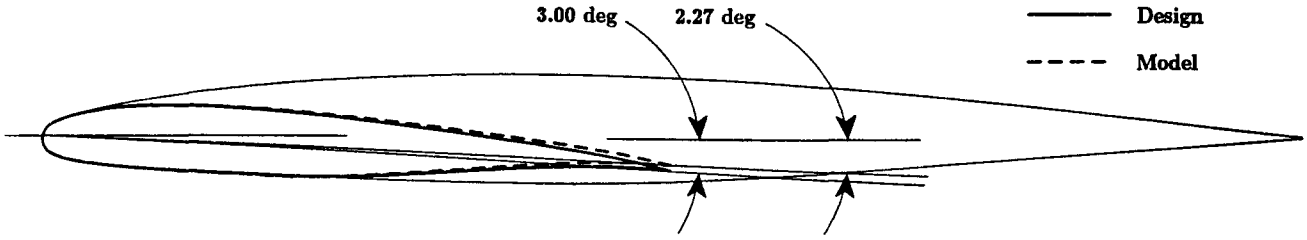

Fig. 3 Nose section overlay plot.

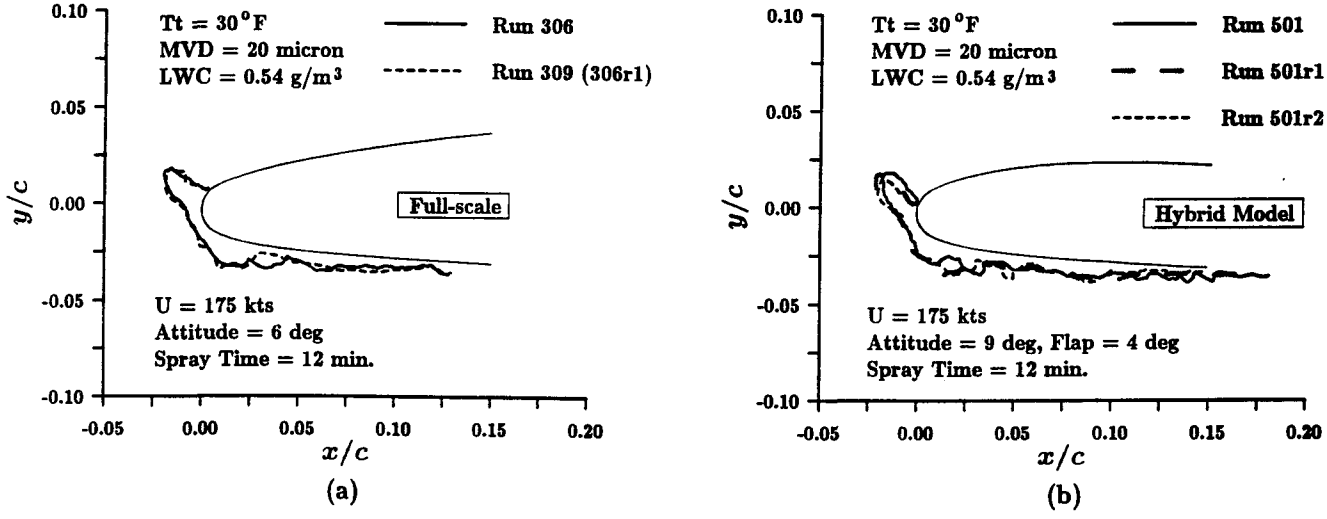

Fig. 4 Ice shape repeatability in the IRT.

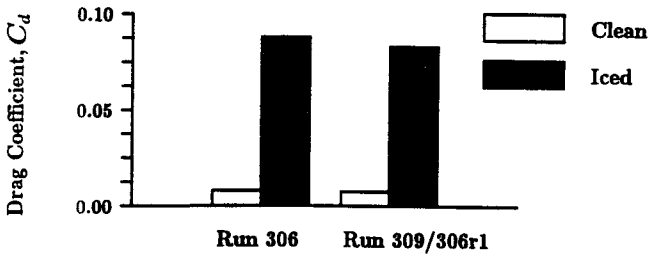

Fig. 5 Repeatability of section drag coefficient for separate test runs before and after ice accretion. (Test conditions shown in Fig. 4a)

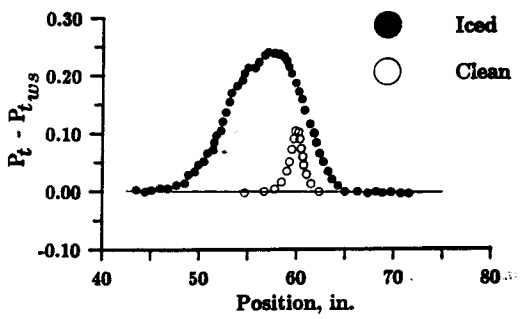

Fig. 6 A comparison of the size of the wake profiles of the clean and iced full-scale airfoil.

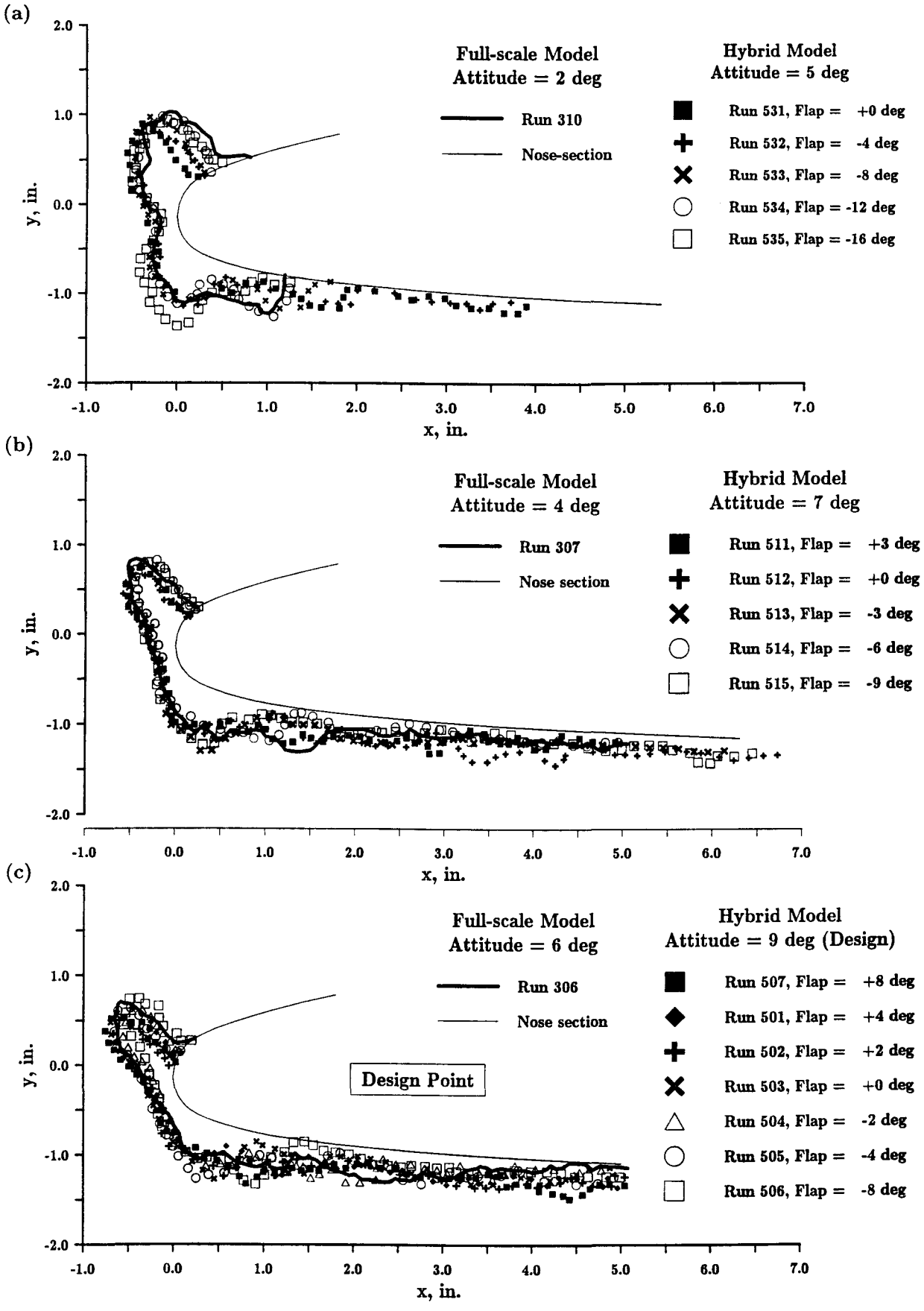

Fig. 7 Comparison of full-scale and hybrid airfoil ice shapes at several angles of attack and at test conditions: Tt = 30 °F, MVD = 20 micron, LWC = 0.54 g/m U = 175 kts, and Spray Time = 12 min.

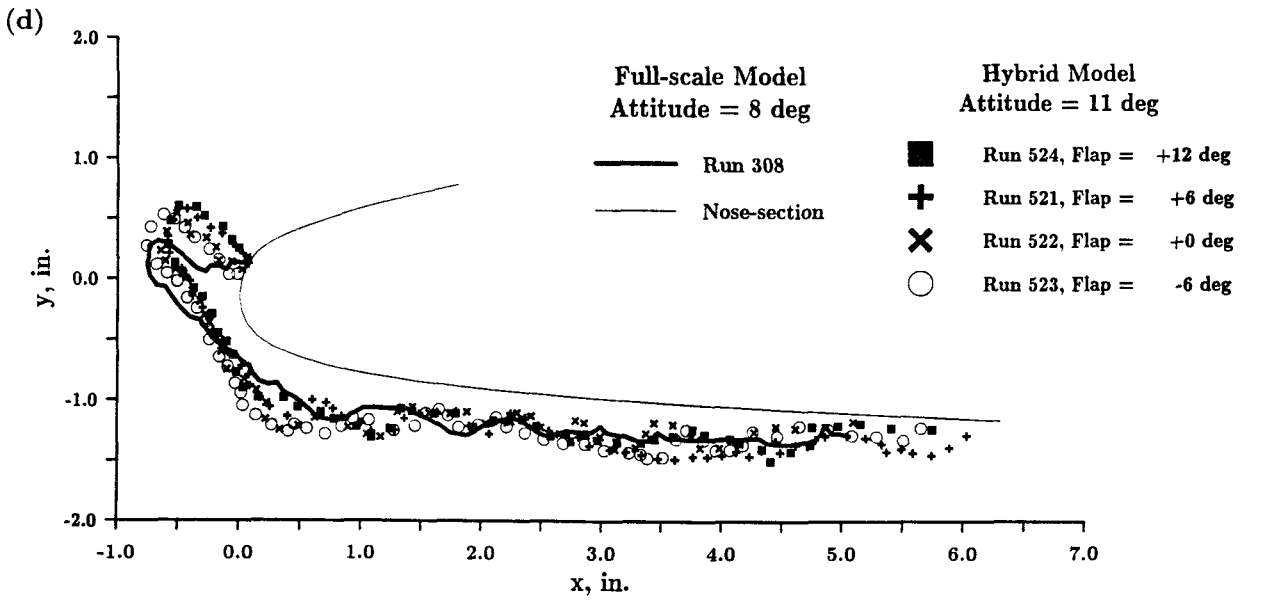

Fig. 7 (continued) Comparison of full-scale and hybrid airfoil ice shapes at several angles of attack and at test conditions: Tt = 30°F, MVD = 20 micron, LWC = 0.54 g/m^3, U = 175 kts, and Spray Time = 12 min.

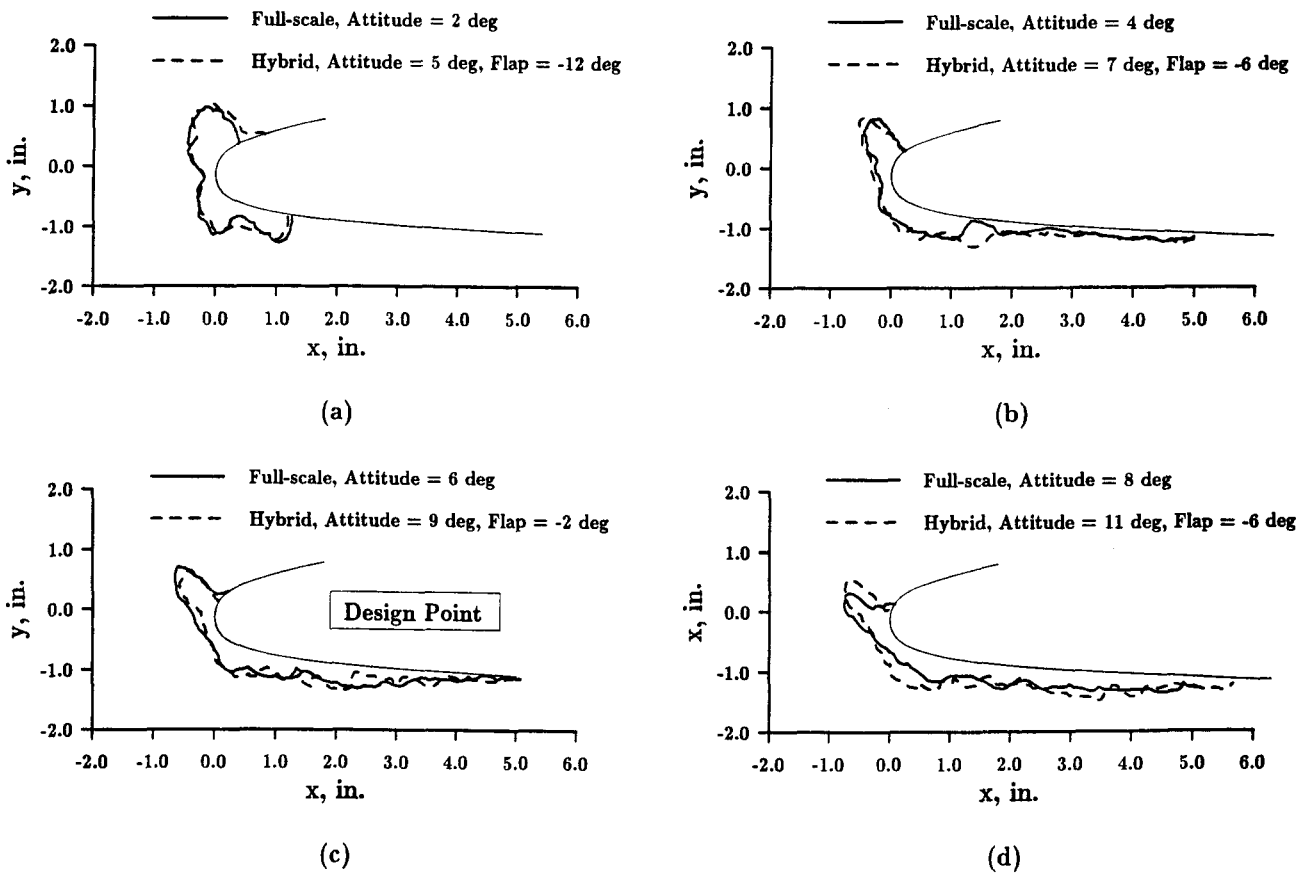

Fig. 8 Plot of hybrid airfoil ice shapes that best simulate the corresponding full-scale ice shapes for the test conditions: Tt = 30°F, MVD = 20 micron, LWC = 0.54 g/m^3, U = 175 kts, and Spray Time = 12 min.

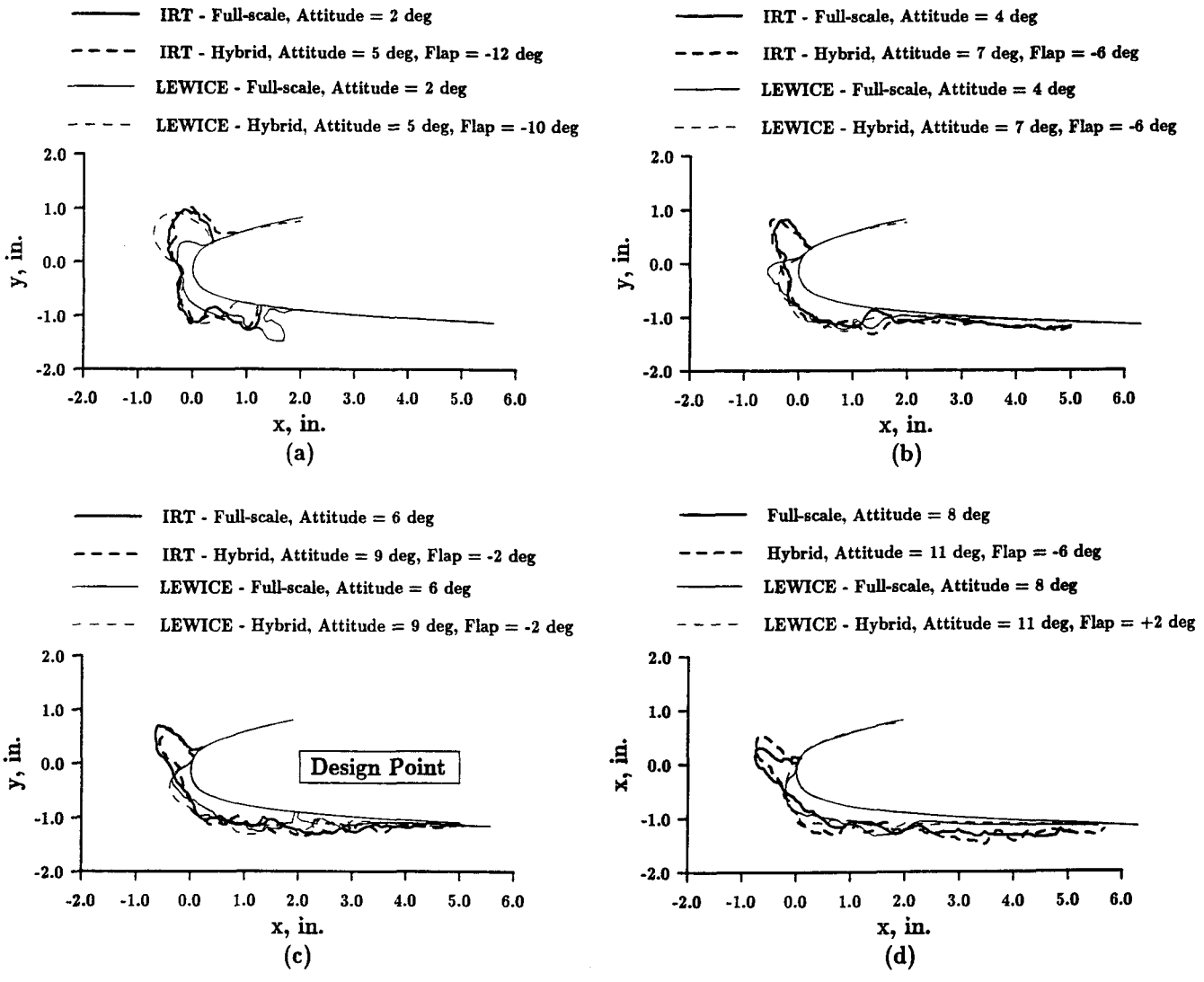

Fig. 9 Comparison of actual ice shapes with LEWICE predictions for the test conditions: Tt = 30°F, MVD = 20 micron, LWC = 0.54 g/m^3, U = 175 kts, and Spray Time = 12 min.

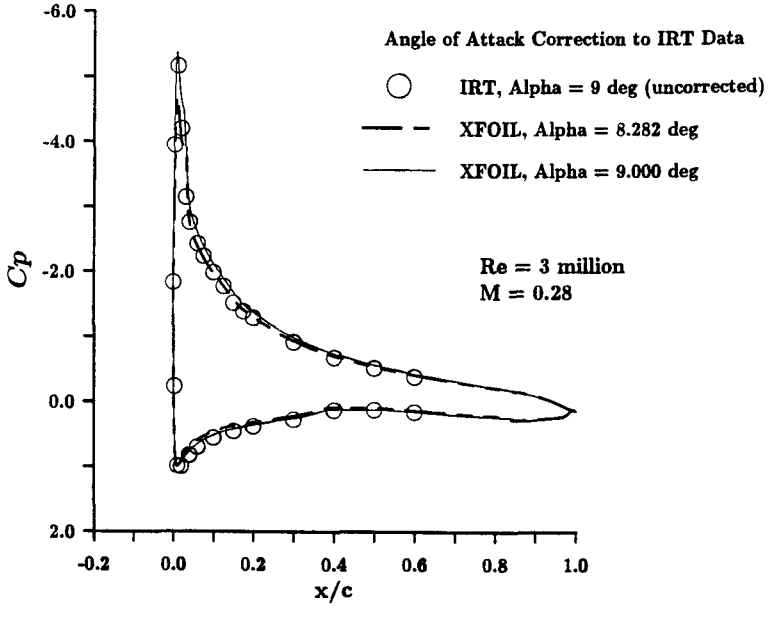

Fig. 10 Comparison of calculated and measured surface pressure distributions on the hybrid model to determine the angle of attack correction to the hybrid airfoil test data.

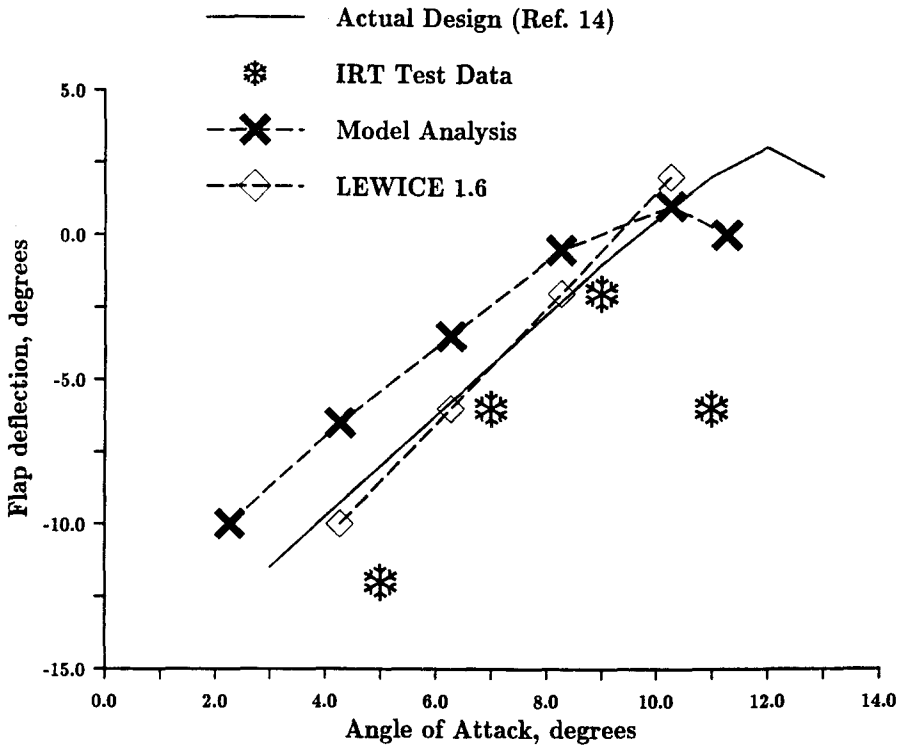

(a) Uncorrected for angle of attack.

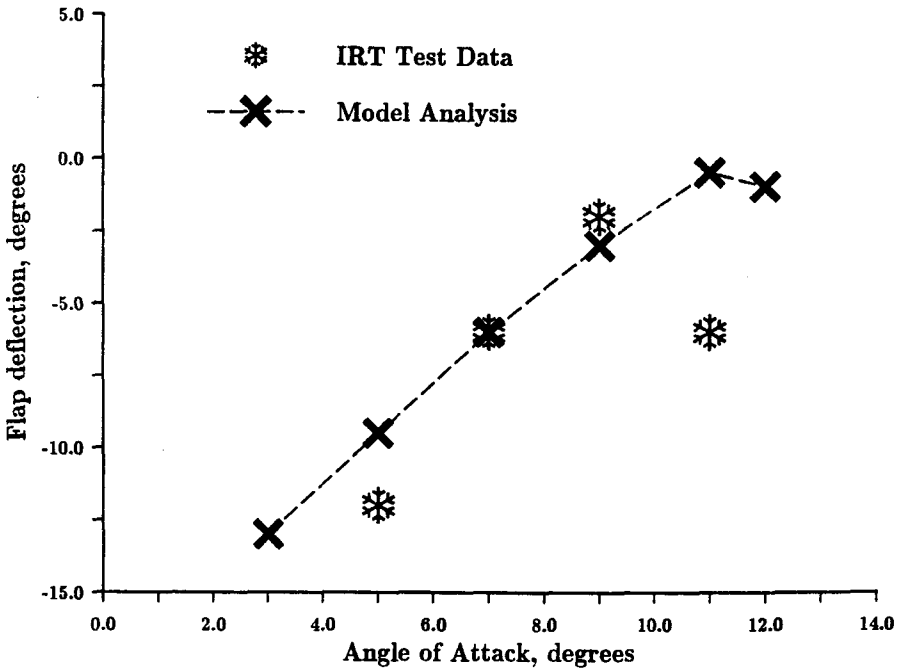

(b) Corrected for angle of attack.

Fig. 11 Plot of the optimum flap deflection from different analyses in comparison with IRT tests data.